Int. J. Electrochem. Sci., 17 **(2022)** Article Number: 220916, doi: 10.20964/2022.09.01

International Journal of
ELECTROCHEMICAL
SCIENCE
www.electrochemsci.org

Short Communication

Degradation of Acid Yellow 36 Azo Dye From Textile Wastewater using Vanadium-doped TiO_2 Photonanocatalyst

Wanhe Yao[1], *Chao Luo*[2,*], *JianBei Wu*[3], *Gongjingyi Hou*[2]

[1] Cnooc Ningbo Daxie Petrochemical Ltd, Ningbo 315812, China；
[2] CenerTech Tianjin Chemical Research and Design Institute Co.，Ltd.，Tianjin 300131，China
[3] CNOOC Huizhou Petrochemicals Company Limited, Huizhou 516086, China;
[*]E-mail: cnooclc@sina.com

Received: 1 May 2022 / *Accepted:* 13 June 2022 / *Published:* 7 August 2022

The current research is focused on the manufacture of TiO_2 and V-doped TiO_2 nanocatalysts by sol-gel and the evaluation of photodegradation performance in the treatment of Acid Yellow 36 (AY36) dye from textile wastewater under visible light irradiation. SEM and XRD investigations revealed that TiO_2 and V-doped TiO2 nanoparticles were produced in a spherical form, with well-crystallized α-V_2O_5 nanostructures inserted in an anatase TiO_2 structure for V-doped TiO_2 nanoparticles. The optical band gap energies of TiO_2 and V-doped TiO2 nanoparticles were found to be 3.08 and 2.22 eV, respectively, in the study optical absorption spectra. Doping V into the TiO_2 structure reduced the optical band gap energy, meaning that V-doped TiO_2 could be used under visible illumination. Electrochemical investigations revealed that the V-doped TiO2 nanocatalyst had a decreased charge resistance and recombination rate. The photodegradation activity for treatment of 150 ml of 5 mg/l AY36 solution revealed that remarkable photodegradation was observed under the first 10 minutes of visible light irradiation for TiO_2 (20%) and V-doped TiO_2 (40%) in the presence of TiO2 and V-doped TiO_2 nanocatalysts, respectively, and total photodegradation was obtained after 75 and 60 minutes of visible light irradiation in the presence of TiO2 and The V-doped TiO_2 was found to be effective in removing AY36 from textile wastewater sources.

Keywords: V-doped TiO_2; Nanocatalysts; Recombination rate; Acid Yellow 36; Photodegradation; Textile wastewater

1. INTRODUCTION

The discharge of azo dye-containing wastewater into the environment today, as a result of urbanization and industrialization, releases hazardous chemicals into the aquatic environment, inhibits light penetration, and degrades the performance of algae and growing aquatic plants [1, 2]. Organics,

nutrients, and pollutants with low concentrations cause the majority of pollution, which is very harmful to humans and the aquatic environment [3, 4].

Acid Yellow 36 (AY36) is a poisonous azo dye also known as Metanil yellow [5-8]. Water-soluble dye AY36 is used in the beverage, leather, paper, and textile industries [9-11]. Furthermore, because of its color, which ranges from yellow to orange, it is commonly used in sweets, beans, and turmeric in India [12, 13]. When the actual curcumin level is low, it has been added to turmeric powder to simulate the appearance of curcumin. Turmeric is used for its therapeutic properties, which are mostly attributed to curcumin. According to animal research, AY36 is neurotoxic and hepatotoxic [14, 15]. When AY36 comes into contact with the skin, it can induce allergic dermatitis, as well as toxic methaemoglobinaemia and cyanosis in humans [16-19]. Studies have been suggested that AY36 shows tumour-producing effects and may lead to intestinal and enzymic disorders in the human body [20, 21].

Accordingly, many treatment techniques such as electro-Fenton and photoelectro-Fenton processes [22, 23], electrochemical oxidation [24-26], anaerobic–aerobic treatment processes [27, 28], electrocoagulation [29], adsorption [30, 31], and photocatalytic degradation processes [32-36] have been studied for the degradation of AY36, dye contaminated wastewater. However, the use of metal-oxide semiconductor nanostructures for the photocatalytic degradation of dyes has many advantages, no study has been conducted on the photocatalytic and electrochemical performance of V-doped TiO_2 nanostructures. Therefore, in this study, TiO_2 and V-doped TiO_2 nanocatalysts were synthesized via the sol-gel technique and applied as photocatalyst to the photodegradation of acid yellow 36 dyes. Furthermore, an electrochemical method was used to reveal the rapid electron transport and higher photodegradation efficiency of a V-doped TiO_2 nanocatalyst.

2. EXPERIMENT

2.1. Preparation TiO_2 and V-doped TiO_2 nanocatalysts

The TiO_2 and V-doped TiO2 nanocatalysts were prepared using the sol-gel technique [37, 38]. The TiO2 nanocatalyst was made by combining a solution of 10 mL of tetraisopropoxide (97%, Merck, Germany), 5 mL of hydrochloric acid (37%, Sigma-Aldrich), and 30 mL of anhydrous ethanol (99%, Shandong Baovi Energy Technology Co., Ltd., China). To create a homogeneous solution, the mixture was ultrasonically sonicated for 15 minutes. A specified amount of vanadium (V) oxytriisopropoxide (99%, Sigma-Aldrich) was added to the resulting solution under vigorous stirring for 20 minutes to generate V/Ti ratios of 2 wt%. The obtained solution was then added to 2.0 g of triblock copolymer (Pluronic P123, Sigma-Aldrich) diluted in 5 mL of ethanol, followed by continuous magnetic stirring for 120 minutes at 28°C. The suspensions containing TiO2 and V-doped TiO2 nanocatalysts were then transferred to an oven and cooked at 90°C for 150 minutes. The suspensions were centrifuged for 15 minutes at 5000 rpm. The precipitates were then calcined for 180 minutes at 450° C.

2.2. Characterizations and instruments

The morphology and structure of the samples were analyzed by scanning electron microscope (SEM, Hitachi S-4700, Japan) and Rigaku RINT-2100 X-ray diffractometer (XRD) system with Cu Kα radiation (λ = 1.5406 Å). A UV-vis spectrophotometer was used to measure absorption spectra (USB4000, Ocean Optics, USA). The electrochemical impedance spectroscopy (EIS) experiments were carried out under visible light illumination using the ZENNIUM electrochemical workstation (ZAHNER-elektrik GmbH & Co. KG, Germany) in a conventional three-electrode system consisting of a saturated Ag/AgCl electrode and Pt wire as reference and counter electrode, respectively. As working electrodes, TiO_2 and V-doped TiO_2 modified Fluorine doped Tin Oxide (FTO, Sigma-Aldrich) were used. The EIS experiments were performed at an amplitude of 5 mV in the frequency range of 10^5 Hz to 10^{-2} Hz at open circuit in 0.5 M Na_2SO_4 (≥99%, Sigma-Aldrich) solution. The EIS data was fitted using equivalent circuits with ZView software.

2.3. Photodegradation experiment

The photocatalytic performance of TiO_2 and V-doped TiO_2 nanocatalysts was evaluated using visible light irradiation of 150 ml of AY36 solution in a cylindrical Pyrex vessel equipped with a 500 W halogen lamp (Cangzhou Xinghan Photoelectric Technology Co., Ltd., China). The sample distance from the light source was 8 cm. Before photodegradation reactions, 15 mg of catalyst was magnetically agitated for one hour in a dark position in 150 ml of produced AY36 solutions with deionized water and an actual sample of textile wastewater (textile industry, Changzhou, China). For photodegradation measurements, the light source was irradiated on samples for a certain time interval, and irradiated samples were centrifuged, and subsequently filtered through a Millipore filter (0.22 μm, MF-Millipore™, Merck, Germany). Then, concentration of AY36 was monitored using UV-vis absorbance (spectrophotometer, JASCO Analytical Instruments, Easton, MD, USA) at λ_{max} = 420 nm [39, 40]. The photodegradation efficiency (η) was calculated by the following equation [41, 42]:

$$\eta\ (\%) = \frac{I_0 - I_t}{I_0} \times 100 = \frac{C_0 - C_t}{C_0} \times 100 \qquad (1)$$

Where I_o and I_t are the absorbance intensities of initial and light irradiated AY36 solutions, respectively, and C_o and C_t is the corresponding AY36 concentrations in initial and light-irradiated AY36 solutions, respectively.

3. RESULTS AND DISCUSSION

3.1. SEM and XRD analyses

Figures 1a and 1b show SEM images of prepared TiO_2 and V-doped TiO_2 nanocatalysts, respectively. As shown in Figure 1a, TiO_2 nanoparticles have a spherical shape with an average diameter of 70 nm. Pure TiO2 nanoparticles have clumped together to form clusters, resulting in a

rough and porous surface. The average diameter of the spherical-shaped -doped TiO_2 nanoparticles is 80 nm, as shown in Figure 1b. Although V doping reduces the size of nanoparticles, the shape of doped nanoparticles remains constant, and there is some agglomeration. The shape of V-doped TiO_2 nanoparticles reveals extremely porous materials with particular surface areas, which can obviously improve light absorption and photocatalytic activity [43-46].

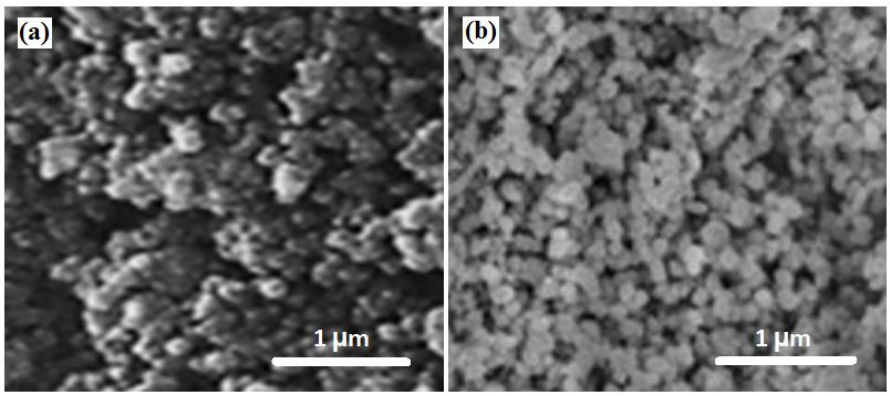

Figure 1. SEM images of prepared (a) TiO_2 and (b) V-doped TiO_2 nanocatalysts.

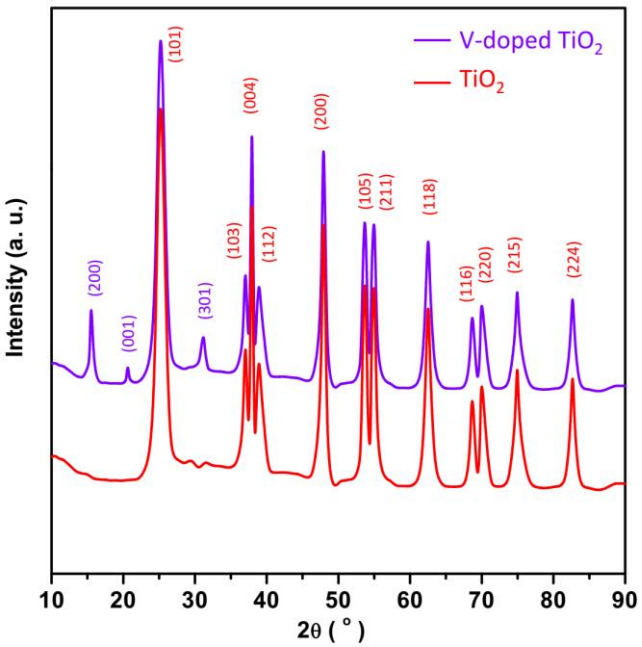

Figure 2. The XRD diffractogram patterns prepared TiO_2 and V-doped TiO_2 nanocatalysts.

Figure 2 shows the XRD diffractogram patterns of TiO2 and V-doped TiO2 nanoparticles. As seen in the diffractogram patterns of TiO2 and V-doped TiO2, the XRD patterns show diffraction peaks at 25.20°, 37.02°, 37.94°, 38.95°, 47.97°, 53.47°, 54.86°, 62.59°, 68.63°, 70.02°, 74.85°, and 82.51°, which correspond to the planes anatase crystalline (JCPDS Card No. 01-078-248) [47-49].

Three additional peaks at 15.53°, 25.62°, and 31.16° on the XRD pattern of V-doped TiO2 nanoparticles are attributed to (200), (001), and (301) orthorhombic -V2O5 phase reflections (JCPDS card no. 41–1426) [50-53], implying that well-crystallized α-V_2O_5 is inserted in anatase TiO_2 structure.

3.2. UV–vis optical absorption spectra

The electronic band structure and optical features such as optical band gap energy (Eg) of photocatalysts are largely dependent on their photocatalytic activity and photodegradation performance [54, 55]. Because TiO_2's large band gap (3.2 eV) permits it to absorb only ultraviolet (UV) light (<387 nm), which accounts for only 4 percent -5 percent of solar radiation, its photocatalytic activity is limited to the UV area [56-58]. Thus, the introduction of metal species such as V is expected to create intra-band gap states and decrease the Eg of TiO_2 to certain extent [59, 60]. Another great problem in using TiO_2 is the fast recombination of photo-excited electrons and holes which results in low photo quantum efficiency [61, 62]. Figure 3a exhibits the UV–vis optical absorption spectra of TiO_2 and V-doped TiO_2 nanoparticles which indicates higher absorption intensity of V-doped TiO_2 nanoparticles in the UV-light region with different absorption tails extending up to the visible region. The absorption edges of V-doped TiO_2 shift to longer wavelengths, which indicates that prepared V-doped TiO_2 by the sol-gel method has the potential to be applied under visible illumination [63, 64]. The absorption spectra of V-doped TiO_2 demonstrates the trace introduction of V which results in the shift the absorption edge to a lower energy, and formation impurities and lattice disorder such as defect energy levels of oxygen vacancies (Vo) located at positions accessible to the bottom of the TiO_2 conduction band can narrow the band-gap which also indicates the formation of gap states [65, 66]. Moreover, the decrease of band gap of V-doped TiO_2 is associated with the overlapping of 3d and 2p orbitals of V and oxygen which initiated the formation of intermediate bands [66-68]. Studies confirmed that V ions can be doped in TiO_2 by substituting Ti^{4+} ions, which act as an intermediate agent for the transfer of photo-generated electrons from the valence band to the conduction band of TiO_2 [66, 69]. The migration of electrons to the conduction and valence bands of V_2O_5 inhibits the recombination of photo-generated charge carriers in TiO_2, enhancing the visible light absorption efficiency of V-doped TiO_2 photocatalysts [70, 71]. In addition, the lower Fermi level of the V_2O_5 species results in V^{5+} species being able to trap photo-generated electrons and leave holes in the valence band and improve the separation of photo-generated electrons and holes on the surface [70, 72, 73].

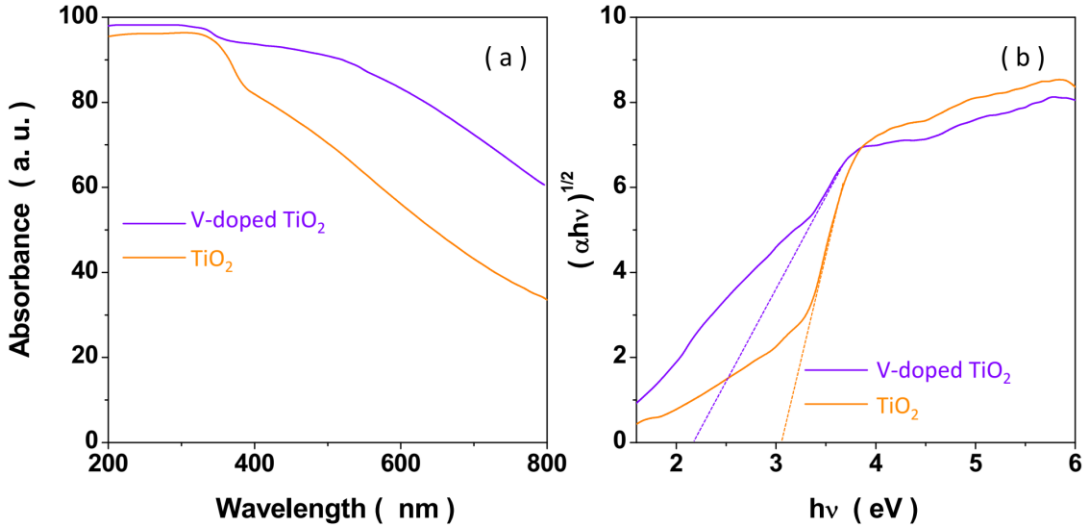

Figure 3. (a) UV–vis optical absorption spectra and (b) Tauc plots of TiO_2 and V-doped TiO_2 nanoparticles.

Figure 3b shows Tauc plots of TiO_2 and V-doped TiO_2 nanoparticles to determine the Eg of the samples which can be calculated using the following equation [74]:

$(\alpha h\nu)^{1/2} = A(h\nu - Eg)$ (2)

Where α and hν are absorption coefficients and photon energy, respectively, and A is constant. The intersection of the extrapolated linear portion of the curve with the hν axis yields Eg values of 3.08 and 2.22 eV for TiO_2 and V-doped TiO_2 nanoparticles, respectively. Eg drops when V is doped into the TiO_2 structure, indicating that V has a major impact on the light absorption properties of the doped sample. The charge transfer transition between the d-electrons of the dopant and the TiO2 conduction band reduces the Eg value, which is attributable to the coexistence of Ti^{4+}, V^{5+}, and Vo in V_2O_5 [75-78].

3.3. Electrochemical analyses

Figures 4a and 4b show the Nyquist and Bode plots of TiO_2 and V-doped TiO_2 nanoparticles, respectively. Table 1 summarizes the parameters obtained by fitting the EIS spectra with the equivalent circuit, which is also shown in Figure 5. Rs denotes the Ohmic internal resistance, Rct_1 denotes charge-transfer resistance at the working electrode/electrolyte interface, Rct2 denotes charge-transfer resistance at the counter electrode/electrolyte interface, and CPE1 and CPE2 denote the working and counter electrodes' constant phase elements, respectively. [79]. The two semicircles in Nyquist plots of both samples indicate that the first semicircle is related to charge transfer resistance at the Pt counter electrode/electrolyte interface at high frequency (Rct_2), and the second semicircle at mid and low frequencies ranges corresponds to the charge-transfer resistance at the TiO_2 based nanocatalyst/electrolyte interface (Rct_1) [80, 81]. Table 1 shows that V-doped TiO_2 nanoparticles possess lower electrochemical impedance to charge transport than that pure TiO_2 sample, indicating the electron transfer from the electrolyte to the V-doped TiO_2 nanoparticles became faster than pure TiO_2

sample, and implying an efficient injection of electrons to doped TiO_2 and decreasing the rate of electron recombination [79]. There are characteristic low frequency peaks (f_{max}) in Bode plots at 25 KHz and 14 KHz for pure TiO_2 and doped TiO_2 samples, respectively. Electron life time (τ) as an important parameter affecting the efficiency of recombination in photocatalytic activity can be determined by f_{max} in Bode plots using the following equation [82, 83]:

$$\tau = \frac{1}{2\pi f_{max}} \quad (3)$$

Recombination is inversely proportional to electron life time. Results indicate that V-doped TiO_2 nanoparticles have a lower recombination possibility than pure TiO_2 samples. Therefore, the lower charge resistance and recombination rate of V-doped TiO_2 nanocatalyst can provide the rapid electron transport and higher photodegradation efficiency [79, 80, 82].

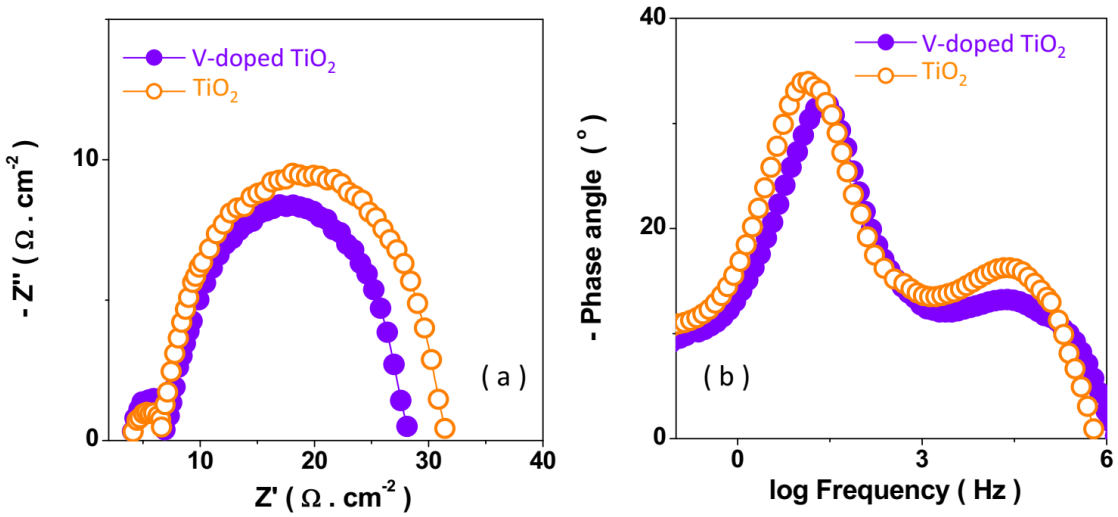

Figures 4. (a) The Nyquist and (b) Bode plots of TiO_2 and V-doped TiO_2 nanoparticles.

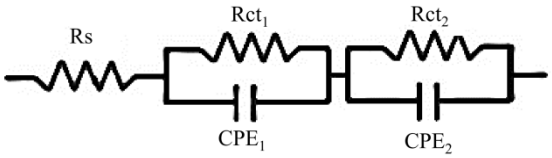

Figures 5. Equivalent circuit.

Table 1. The parameters obtained by fitting the EIS spectra

Sample	**Rs (Ω.cm^{-2})**	**Rct$_1$ (Ω.cm^{-2})**	**Rct$_2$ (Ω.cm^{-2})**
TiO_2	4.61	2.6	25.7
V-doped TiO_2	4.46	2.0	20.9

3.4. Photodegradation activity

Figure 6 shows the findings of the research of TiO2 and V-doped TiO2 photodegradation performance in the degradation of 150 ml of 5 mg/l AY36 solution in darkness (first hour) and under visible light irradiation. During dark conditions, photocatalysts and control samples (without photocatalyst) have an insignificant photodegradation efficiency (less than 0.5%). After 2 hours of visible light irradiation, the photodegradation efficiency of the control sample is very low (≤ 1.2%). Meanwhile, substantial photodegradation is found for TiO2 (20%) and V-doped TiO2 (40%) after 10 minutes of visible light irradiation, showing important roles for visible light and photocatalysts in AY36 solution degradation. Results in Figure 6 also reveal that total photodegradation is obtained after 75 and 60 minutes of visible light irradiation in the presence of TiO_2 and V-doped TiO_2 nanocatalysts, respectively. Therefore, the V-doped TiO_2 exhibits a higher rate of AY36 degradation, which can be related to its larger specific surface area that clearly can enhance the active sites, light absorbance and photocatalytic performance [43, 84]. Moreover, the better photocatalytic degradation of AY36 on V-doped TiO_2 nanocatalyst may be associated with its better photo-generated electron-hole separation and rapid charge transfer than pure TiO_2 nanocatalyst. The photo-generated holes can act as strong oxidizing agents or form powerful oxidizing agents hydroxyl radicals (OH·) by reacting with water molecules or hydroxyl groups on the nanocatalyst surface which initiates the dye degradation process [85]. Whereas photo-generated electrons react with the oxygen to form anionic superoxide radicals (O^{-}_2) [36]. In addition, V doping in TiO_2 matrix narrows the band gap and creates impurity states which act as the ladder for transferring electrons or act as trap centers for photogenerated electrons and holes. These lead to an increase in the lifetime of the photo-generated charges [86], evidenced to enhance the photocatalytic activity which is in good agreement with SEM, optical and EIS results.

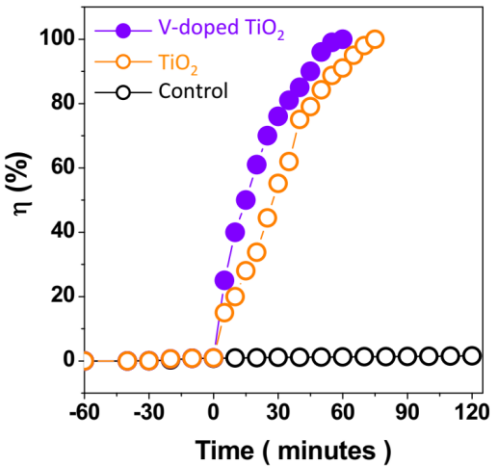

Figure 6. Photodegradation performance of TiO_2 and V-doped TiO_2 for the degradation of 150 ml of 5 mg/l AY36 solution in darkness (first hour) and under visible light irradiation.

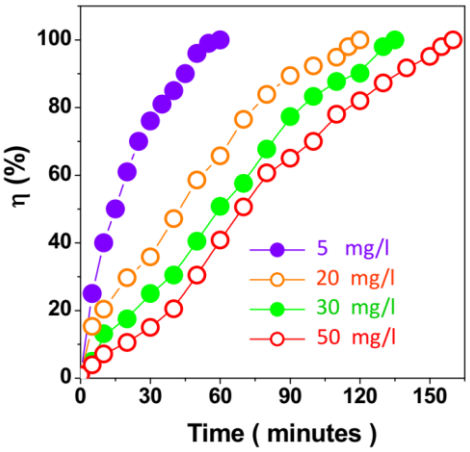

Figure 7. Photodegradation performance of V-doped TiO_2 for the degradation of 150 ml of different initial concentrations (5, 20, 30 and 50 mg/l) of AY36 solution under visible light irradiation

The effect of different initial concentrations of AY36 solution (5, 20, 30, and 50 mg/l) on the photodegradation performance of V-doped TiO_2 was investigated. Figure 7 shows that as the initial AY36 concentration increases, the photodegradation efficiency declines dramatically, and total degradation of 5, 20, 30, and 50 mg/l of AY36 is reached after 60, 120, 135 and 160 minutes of visible light irradiation, respectively. Table 2 compares the photodegradation performance of the V-doped TiO_2 photocatalyst in this study to other photocatalysts reported in the literature for the removal of AY36, demonstrating that the V-doped TiO2 photocatalyst has a high photodegradation efficiency due to the formation of intermediate states in the semiconductor's energy band-gap, effectively narrowing the band gap and increasing the photo-generated charge carry life time [87, 88].

Table 2. Comparison between photodegradation performance of V-doped TiO_2 photocatalyst in present study and other reported photocatalysts in the literature for the removal of AY36.

Photocatalyst	**AY36 content (mg/l)**	**Light source**	**Degradation time (minute)**	**η(%)**	**Ref.**
V-doped TiO_2	50	Simulated sunlight	160	100	This work
	30		135	100	
	20		120	100	
	5		60	100	
ZnO	50	UV	180	97	[33]
TiO_2 coupled photocatalytic membrane	30	UV	300	42	[32]
TiO_2 P25 coupled photocatalytic membrane	30	UV	300	32	[35]
TiO_2	20	UV	1680	88.4	[34]
TiO_2 P25	5	UV	105	84.3	[36]

The ability of V-doped TiO2 to photodegrade AY36 in real-world textile wastewater (TW) samples was examined. Figures 8 and 9 show the photodegradation efficacy of 150 ml of 5 mg/l AY36 solutions made from TW samples and deionized water (DW) as a control sample when exposed to visible light. Total AY36 degradation took 60 and 78 minutes in the control and TW samples, respectively, indicating that the longer time (18 minutes) required for 100% AY36 treatment in the textile wastewater sample was associated with the presence of additional AY36 and other pollutants molecules in textile wastewater. Furthermore, the results demonstrate the effectiveness of V-doped TiO2 in removing AY36 from textile wastewater sources.

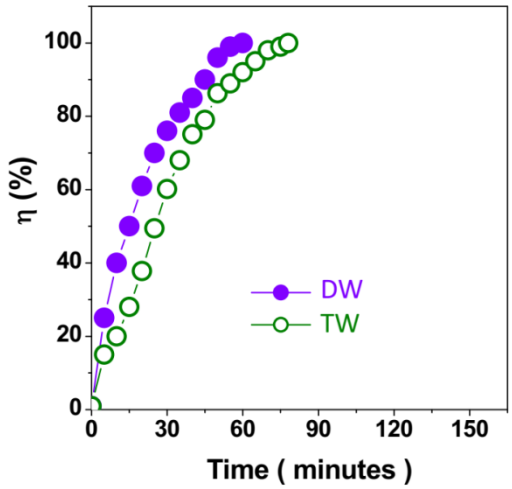

Figure 8. The photodegradation effectiveness of 150 ml of 5 mg/l AY36 solutions made from textile wastewater (TW) sample and deionized water (DW) as control sample under visible light irradiation

4. CONCLUSION

This research focused on the synthesis, structural, and optical characterization of TiO_2 and V-doped TiO_2 nanocatalysts, as well as the photodegradation performance of AY36 dye from textile effluent when exposed to visible light. The TiO_2 and V-doped TiO_2 nanocatalysts were prepared using the sol-gel technique. Structural and morphological analyses showed that TiO_2 and V-doped TiO_2 nanoparticles were synthesized in a spherical shape and for V-doped TiO_2 nanoparticles, well-crystallized α-V_2O_5 nanostructures were inserted into the anatase TiO_2 structure. UV–vis optical absorption spectra revealed that doping V into the TiO_2 structure reduced optical band gap energy, meaning that V-doped TiO_2 could be used under visible illumination. Electrochemical analyses revealed that V-doped TiO_2 nanoparticles had a lower electrochemical impedance to charge transport than pure TiO_2 nanoparticles, implying that electron transfer from the electrolyte to the V-doped TiO_2 nanoparticles was faster, implying an efficient injection of electrons into doped TiO_2 and a lower rate of electron recombination. Total photodegradation was obtained after 75 and 60 minutes of visible light irradiation in the presence of TiO_2 and V-doped TiO_2 nanocatalysts, respectively, demonstrating

that visible light and photocatalysts play important roles in the degradation of AY36 solution. The V-doped TiO_2 was found to be effective in removing AY36 from textile wastewater sources.

References

1. P.O. Bankole, A.A. Adekunle and S.P. Govindwar, *Journal of Environmental Chemical Engineering*, 6 (2018) 1589.
2. L. Zhang, L. Wang, Y. Zhang, D. Wang, J. Guo, M. Zhang and Y. Li, *Environmental research*, 206 (2022) 112629.
3. H. Maleh, M. Alizadeh, F. Karimi, M. Baghayeri, L. Fu, J. Rouhi, C. Karaman, O. Karaman and R. Boukherroub, *Chemosphere*, (2021) 132928.
4. C. Liu and J. Rouhi, *RSC Advances*, 11 (2021) 9933.
5. D. Garg, S. Kumar, K. Sharma and C. Majumder, *Groundwater for Sustainable Development*, 8 (2019) 512.
6. X. Tang, J. Wu, W. Wu, Z. Zhang, W. Zhang, Q. Zhang, W. Zhang, X. Chen and P. Li, *Analytical chemistry*, 92 (2020) 3563.
7. T. Gao, C. Li, Y. Zhang, M. Yang, D. Jia, T. Jin, Y. Hou and R. Li, *Tribology International*, 131 (2019) 51.
8. M. Akbari and R. Elmi, *Case reports in medicine*, 2017 (2017) 1.
9. M.E. Farshchi, H. Aghdasinia and A. Khataee, *Water research*, 151 (2019) 203.
10. X. Guo, J. Lu, P. Lai, Z. Shen, W. Zhuang, Z. Han, L. Zhang and S. Lozano-Perez, *Corrosion Science*, 202 (2022) 110300.
11. A. Abdul Rahman–Al Ezzi, *International Journal of Engineering*, 33 (2020) 2120.
12. T. Bigdeli and F. Motiee, *Journal of Environmental Health Engineering*, 7 (2019) 69.
13. W. Liu, F. Huang, Y. Liao, J. Zhang, G. Ren, Z. Zhuang, J. Zhen, Z. Lin and C. Wang, *Angewandte Chemie*, 120 (2008) 5701.
14. S. Samarghandian, M. Azimi-Nezhad, A.M.P. Shahri and T. Farkhondeh, *Acta Bio Medica: Atenei Parmensis*, 90 (2019) 533.
15. G. Li, H. Yuan, J. Mou, E. Dai, H. Zhang, Z. Li, Y. Zhao, Y. Dai and X. Zhang, *Composites Communications*, 29 (2022)
16. O. Anjaneya, S.Y. Souche, M. Santoshkumar and T. Karegoudar, *Journal of Hazardous Materials*, 190 (2011) 351.
17. F. Yu, Z. Zhu, C. Li, W. Li, R. Liang, S. Yu, Z. Xu, F. Song, Q. Ren and Z. Zhang, *Applied Catalysis B: Environmental*, 314 (2022) 121467.
18. H. Karimi-Maleh, R. Darabi, M. Shabani-Nooshabadi, M. Baghayeri, F. Karimi, J. Rouhi, M. Alizadeh, O. Karaman, Y. Vasseghian and C. Karaman, *Food and Chemical Toxicology*, 162 (2022) 112907.
19. M. Khosravi, *Journal of Eating Disorders*, 8 (2020) 1.
20. M.A. Rahman, A.K. Bala, M.A. Rahman, M.K. Hasan and R. Masuma, *Jahangirnagar University Journal of Biological Sciences*, 8 (2019) 35.
21. H. Liu, J. Yang, Y. Jia, Z. Wang, M. Jiang, K. Shen, H. Zhao, Y. Guo, Y. Guo and L. Wang, *Environmental Science & Technology*, 55 (2021) 10734.
22. K. Cruz-González, O. Torres-López, A. García-León, J. Guzmán-Mar, L. Reyes, A. Hernández-Ramírez and J. Peralta-Hernández, *Chemical Engineering Journal*, 160 (2010) 199.
23. C. Espinoza, J. Romero, L. Villegas, L. Cornejo-Ponce and R. Salazar, *Journal of hazardous materials*, 319 (2016) 24.
24. M. Villanueva-Rodríguez, A. Hernández-Ramírez, J. Peralta-Hernández, E.R. Bandala and M.A. Quiroz-Alfaro, *Journal of hazardous materials*, 167 (2009) 1226.

25. X. Tian, R. Yang, T. Chen, Y. Cao, H. Deng, M. Zhang and X. Jiang, *Journal of Hazardous Materials*, 426 (2022) 128121.
26. L. Nan, C. Yalan, L. Jixiang, O. Dujuan, D. Wenhui, J. Rouhi and M. Mustapha, *RSC Advances*, 10 (2020) 27923.
27. R. Ahmad, P.K. Mondal and S.Q. Usmani, *Bioresource technology*, 101 (2010) 3787.
28. M. El-Wazery, *International Journal of Engineering*, 34 (2021) 2418.
29. M. Kashefialasl, M. Khosravi, R. Marandi and K. Seyyedi, *International Journal of Environmental Science and Technology:(IJEST)*, 2 (2006) 365.
30. P.K. Malik, *Dyes and pigments*, 56 (2003) 239.
31. Z. Feng, G. Li, X. Wang, C.J. Gómez-García, J. Xin, H. Ma, H. Pang and K. Gao, *Chemical Engineering Journal*, 445 (2022) 136797.
32. S. Mozia, A.W. Morawski, M. Toyoda and T. Tsumura, *Chemical Engineering Journal*, 150 (2009) 152.
33. S. Khezrianjoo and H.D. Revanasiddappa, *Journal of Catalysts*, 2013 (2013) 1.
34. P. Palak, S. Chauhan, K. Kumar and A. Haritash, *Applied Chemical Engineering*, 2 (2019) 1.
35. S. Mozia, M. Tomaszewska and A.W. Morawski, *Catalysis Today*, 129 (2007) 3.
36. M. Nokandeh and B. Khoshmanesh, *Anthropogenic Pollution Journal*, 3 (2019) 10.
37. P.-Y. Chang, C.-H. Huang and R.-a. Doong, *Water Science and Technology*, 59 (2009) 523.
38. C. Suwanchawalit and S. Wongnawa, *Journal of Nanoparticle Research*, 12 (2010) 2895.
39. T.G. Merlain, L.T. Nanganoa, B.B.P. Desire, N.J. Nsami and K.J. Mbadcam, *Advances in Chemical Engineering and Science*, 6 (2016) 553.
40. J. Rouhi, S. Kakooei, S.M. Sadeghzadeh, O. Rouhi and R. Karimzadeh, *Journal of Solid State Electrochemistry*, 24 (2020) 1599.
41. E. El-Ashtoukhy, N. Amin and M. Abdel-Aziz, *International Journal of Electrochemical Science*, 7 (2012) 11137.
42. A. Alhadhrami, A. Almalki, A.M.A. Adam and M.S. Refat, *International Journal of Electrochemical Science*, 13 (2018) 6503.
43. G. Nagaraj, M.K. Mohammed, H.G. Abdulzahraa, P. Sasikumar, S. Karthikeyan and S. Tamilarasu, *Applied Physics A*, 127 (2021) 1.
44. M.-R. Wang, L. Deng, G.-C. Liu, L. Wen, J.-G. Wang, K.-B. Huang, H.-T. Tang and Y.-M. Pan, *Organic letters*, 21 (2019) 4929.
45. S. Guo, C. Li, Y. Zhang, Y. Wang, B. Li, M. Yang, X. Zhang and G. Liu, *Journal of Cleaner Production*, 140 (2017) 1060.
46. S. Haddadi, R. Shahrokhirad, M.M. Ansar, S. Marzban, M. Akbari and A. Parvizi, *Anesthesiology and pain medicine*, 8 (2018)
47. H. Kaur, V. Goyal, J. Singh, S. Kumar and M. Rawat, *Micro & Nano Letters*, 14 (2019) 1229.
48. Y. Duan, H. Fu, L. Zhang, R. Gao, Q. Sun, Z. Chen and H. Du, *Composites Communications*, 31 (2022) 101106.
49. R. Mohamed, J. Rouhi, M.F. Malek and A.S. Ismail, *International Journal of Electrochemical Science*, 11 (2016) 2197.
50. K.S. Prasad, C. Shivamallu, G. Shruthi and M. Prasad, *ChemistrySelect*, 3 (2018) 3860.
51. M. Yang, C. Li, Y. Zhang, D. Jia, R. Li, Y. Hou, H. Cao and J. Wang, *Ceramics International*, 45 (2019) 14908.
52. H. Karimi-Maleh, C. Karaman, O. Karaman, F. Karimi, Y. Vasseghian, L. Fu, M. Baghayeri, J. Rouhi, P. Senthil Kumar and P.-L. Show, *Journal of Nanostructure in Chemistry*, (2022) 1.
53. M. Khosravi, *Health Psychology Research*, 8 (2020) 91.
54. X. Meng, N. Yun and Z. Zhang, *The Canadian Journal of Chemical Engineering*, 97 (2019) 1982.
55. Y. Fu, H. Chen, R. Guo, Y. Huang and M.R. Toroghinejad, *Journal of Alloys and Compounds*, 888 (2021) 161507.

56. X. Li, D. Wang, Q. Luo, J. An, Y. Wang and G. Cheng, *Journal of Chemical Technology & Biotechnology: International Research in Process, Environmental & Clean Technology*, 83 (2008) 1558.
57. A. Jahanbakhsh, M. Hosseini, M. Jahanshahi and A. Amiri, *International Journal of Engineering*, 35 (2022) 988.
58. M. Akbari, R. Moghadam, R. Elmi, A. Nosrati, E. Taghiabadi and N. Aghdami, *Journal of Ophthalmic and Vision Research*, 14 (2019) 400.
59. M. Motola, L. Satrapinskyy, M. Čaplovicová, T. Roch, M. Gregor, B. Grančič, J. Greguš, Ľ. Čaplovič and G. Plesch, *Applied Surface Science*, 434 (2018) 1257.
60. T. Gao, C. Li, M. Yang, Y. Zhang, D. Jia, W. Ding, S. Debnath, T. Yu, Z. Said and J. Wang, *Journal of Materials Processing Technology*, 290 (2021) 116976.
61. C. Heshan, L. Guoguang, W. Lü, L. Xiaoxia, Y. Lin and L. Daguang, *Journal of Rare Earths*, 26 (2008) 71.
62. M. Hu, Y. Wang, Z. Yan, G. Zhao, Y. Zhao, L. Xia, B. Cheng, Y. Di and X. Zhuang, *Journal of Materials Chemistry A*, 9 (2021) 14093.
63. W. Zhou, Q. Liu, Z. Zhu and J. Zhang, *Journal of Physics D: Applied Physics*, 43 (2010) 035301.
64. Y. Wang, C. Li, Y. Zhang, M. Yang, B. Li, L. Dong and J. Wang, *International Journal of Precision Engineering and Manufacturing-Green Technology*, 5 (2018) 327.
65. A.Y. Choi and C.-H. Han, *Journal of Nanoscience and Nanotechnology*, 14 (2014) 8070.
66. B. Liu, X. Wang, G. Cai, L. Wen, Y. Song and X. Zhao, *Journal of hazardous materials*, 169 (2009) 1112.
67. P. Andami, A. Zinatizadeh, M. Feyzi, H. Zangeneh, S. Azizi, L. Norouzi and M. Maaza, *International Journal of Engineering*, 35 (2022) 351.
68. M. Khosravi, *Pharmacopsychiatry*, 55 (2022) 16.
69. T.-D. Pham and B.-K. Lee, *Applied Surface Science*, 296 (2014) 15.
70. X. Wang, Z. Li, L. Jia and X. Xing, *Journal of the Korean Physical Society*, 72 (2018) 1214.
71. G. Li, S. Huang, N. Zhu, H. Yuan and D. Ge, *Journal of Hazardous Materials*, 403 (2021) 123981.
72. H. Li, Y. Zhang, C. Li, Z. Zhou, X. Nie, Y. Chen, H. Cao, B. Liu, N. Zhang and Z. Said, *Korean Journal of Chemical Engineering*, 39 (2022) 1107.
73. A. Baradaran-Rafii, M. Akbari, E. Shirzadeh and M. Shams, *Journal of ophthalmic & vision research*, 10 (2015) 90.
74. H.S. Abdulla and A.I. Abbo, *International Journal of Electrochemical Science* 7(2012) 10666.
75. M.M. Islam, T. Bredow and A. Gerson, *ChemPhysChem*, 12 (2011) 3467.
76. Z. Wang, Q. Lei, Z. Wang, H. Yuan, L. Cao, N. Qin, Z. Lu, J. Xiao and J. Liu, *Chemical Engineering Journal*, 395 (2020) 125180.
77. H. Karimi-Maleh, H. Beitollahi, P.S. Kumar, S. Tajik, P.M. Jahani, F. Karimi, C. Karaman, Y. Vasseghian, M. Baghayeri and J. Rouhi, *Food and Chemical Toxicology*, (2022) 112961.
78. R.S. Moghadam, M. Akbari, Y. Alizadeh, A. Medghalchi and R. Dalvandi, *Middle East African Journal of Ophthalmology*, 26 (2019) 11.
79. V.-D. Dao and H.-S. Choi, *Nanomaterials*, 6 (2016) 70.
80. H. Ju, J. Wu and Y. Xu, *Journal of Chemical Sciences*, 125 (2013) 687.
81. W. Liu, J. Li, J. Zheng, Y. Song, Z. Shi, Z. Lin and L. Chai, *Environmental Science & Technology*, 54 (2020) 11971.
82. R. Yew, S.K. Karuturi, J. Liu, H.H. Tan, Y. Wu and C. Jagadish, *Optics Express*, 27 (2019) 761.
83. D. Ge, H. Yuan, J. Xiao and N. Zhu, *Science of The Total Environment*, 679 (2019) 298.
84. Y. Yu, X. Yi, J. Zhang, Z. Tong, C. Chen, M. Ma, C. He, J. Wang, J. Chen and B. Chen, *Catalysis Science & Technology*, 11 (2021) 5125.

85. G. Mishra and M. Mukhopadhyay, *Scientific reports*, 9 (2019) 1.
86. P. Zhou, J. Yu and Y. Wang, *Applied Catalysis B: Environmental*, 142-143 (2013) 45.
87. W. Zhu, X. Qiu, V. Iancu, X.-Q. Chen, H. Pan, W. Wang, N.M. Dimitrijevic, T. Rajh, H.M. Meyer III and M.P. Paranthaman, *Physical review letters*, 103 (2009) 226401.
88. W. Yang, H. Zhang, Y. Liu, C. Tang, X. Xu and J. Liu, *RSC Advances*, 12 (2022) 14435.